

Image Comes Dancing with Collaborative Parsing-Flow Video Synthesis

Bowen Wu*, Zhenyu Xie*, Xiaodan Liang[†], Yubei Xiao, Haoye Dong, Liang Lin

Abstract—Transferring human motion from a source to a target person poses great potential in computer vision and graphics applications. A crucial step is to manipulate sequential future motion while retaining the appearance characteristic. Previous work has either relied on crafted 3D human models or trained a separate model specifically for each target person, which is not scalable in practice. This work studies a more general setting, in which we aim to learn a *single* model to parsimoniously transfer motion from a source video to any target person given only one image of the person, named as Collaborative Parsing-Flow Network (CPF-Net). The paucity of information regarding the target person makes the task particularly challenging to faithfully preserve the appearance in varying designated poses. To address this issue, CPF-Net integrates the structured human parsing and appearance flow to guide the realistic foreground synthesis which is merged into the background by a spatio-temporal fusion module. In particular, CPF-Net decouples the problem into stages of human parsing sequence generation, foreground sequence generation and final video generation. The human parsing generation stage captures both the pose and the body structure of the target. The appearance flow is beneficial to keep details in synthesized frames. The integration of human parsing and appearance flow effectively guides the generation of video frames with realistic appearance. Finally, the dedicated designed fusion network ensure the temporal coherence. We further collect a large set of human dancing videos to push forward this research field. Both quantitative and qualitative results show our method substantially improves over previous approaches and is able to generate appealing and photo-realistic target videos given any input person image. All source code and dataset will be released at <https://github.com/xiezhy6/CPF-Net>.

Index Terms—Motion Transfer, Video Synthesis, Generative Model

I. INTRODUCTION

Transferring human motion from one subject to another target subject is a long-standing challenge in computer vision and graphics. Such techniques enable us to generate animations and videos of a human with realistic motion and appearance, and can be particularly useful in virtual reality, video games, art creation, and so forth. A crucial part of the problem is modeling the characteristics (e.g., body shape, clothing appearance) of the target subject. Previous research has studied settings of using 3D human models to this end [9], [15], [35], [46]. Recent work [7] instead learns a personalized neural network from videos of each target subject, which is then used to synthesize new videos of arbitrary motions of the particular target person. Despite the impressive results,

however, both the 3D character models and the subject-specific neural models can hardly scale up in practice. For example, consider deploying an application of creating dancing videos for any users on social media, it is computationally and economically prohibitive to train a model for each user.

In this work, we consider a more practical setting of using a *single* model to transfer motions to any target person based on only *one image* of the person. The image provides the appearance characteristics of the target subject. With this image and a video of source subject, we aim to synthesize a realistic video wherein the target performs the same motions as in the source video. Figure 1 illustrates our task. Applying the same model for everybody and requiring only a single target image can enable very scalable applications, simultaneously also imposes unique technical challenges in generating photo-realistic videos with faithful target appearance and smooth designated motions.

In contrast to previous settings where videos of a target subject provide rich person information and end-to-end neural models can straightforwardly be applied [48], a solution to this task must ensure accurate modeling of the target subject despite the paucity of information from the single image, and the model must be applicable to any given target subject without specific training. This necessitates a structured method that incorporates the human body and motion structures for effective motion transferring.

To address the above mentioned challenges, we propose a Collaborative Parsing-Flow method (CPF-Net) that integrates structured human parsing and appearance flow to guide the video synthesis. Specifically, a human parsing, as a semantic segmentation of human parts (e.g., head, legs, etc) [24], [25], [26], [52], [12], effectively captures both the pose and the structure of the target person, which can not only guide to generate video frames of the target in various poses but guide the generator to synthesize different body part precisely. The appearance flow, indicating the pixel corresponding relation between the source and target image, can be used to warp the source appearance to the target shape and keep the source image appearance details as much as possible. In particular, we decompose the problem into three stages, namely, pose-guided human parsing synthesis, parsing-flow-guided foreground synthesis, and spatio-temporal fusion-based video synthesis. In the first stage, we generate a sequence of the target’s human parsing conditioning on the pose of the source video and the appearance parsing of the target person. In the second stage, we first utilize a flow regression network to estimate a appearance flow between the appearance pose and each source video pose, which is used to warp the extracted feature of the

* Bowen Wu and Zhenyu Xie contribute equally to this work

[†] Corresponding author: Xiaodan Liang, E-mail: xdliang328@gmail.com

All authors are with Sun Yat-sen University, China. Liang Lin is also with Dark Matter AI Research, China.

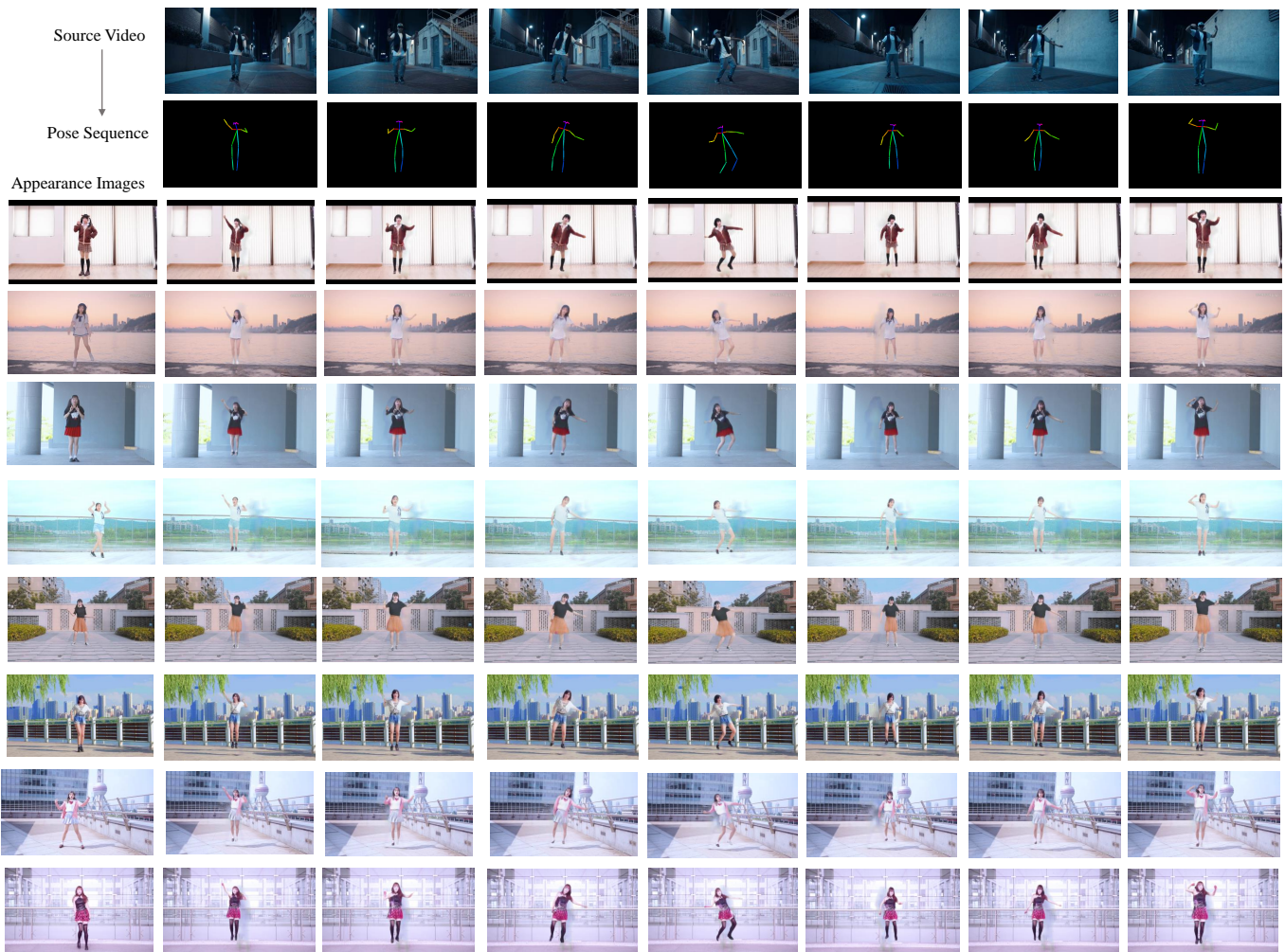


Fig. 1: **Synthesized Videos of Our Approach.** Given an appearance image of a target person and a video of a source person, our model generates a video of the target person which retains the source video motions. The first column is the appearance images of three target persons. The first two rows are the source video and its estimated pose sequence, respectively. The next three rows are the synthesized video frames via both retaining the target person’s appearance and the source video motions.

appearance foreground. Collaborating the human parsing and warped appearance feature, the target foreground is generated. In the third stage, the foreground and background are fused together while keeping the temporal smoothness by taking the previous synthesized frame as the input of the fusion network.

To push the limit of the arbitrary human motion transfer research field, we further build a large collection of dancing videos. The dataset consists of 428 videos of different people performing various dances in diverse scenes. We conduct extensive experiments to compare with strong baselines adapted from previous approaches [49], [48], [10]. Both quantitative and qualitative results demonstrate the superiority of the proposed method. Figure 3 and Figure 4 show our method gains much better visual quality compared with existing baseline methods.

II. RELATED WORK

A. Motion Transfer

Extensive works [9], [15], [35], [46], [7], [27], [38] of motion transfer have been done in the past decades and are widely used in various areas. Liu *et al.* [27] has explored to build a motion transfer system based on a rough 3D human model. Villegas *et al.* attempted to transfer motions from a source to any 3D target characters with forward kinematics and inverse kinematics.

All of the above methods have achieved positive results but they must be supported by 3D models which are difficult to be acquired and complex. Instead, our proposed CPF-Net is free of fine-grained 3D character models and only requires one image of the target person to transfer motions from source video to the target person. Breaking through the limitations of 3D models, a very recent work [7] proposed a framework based on pix2pixHD [17] to straightforwardly train an end-to-end neural network that can transform 2D pose to the target

person. However, it needs to train a personalized model for each target person. Opposed to it, another family of methods called image animation [40], [39], [44] could animate any source object according to the motion of a driving video in single model. MoCoGAN [44] maps a sequence of video frames to a sequence of random vectors. Motion transfer can be realized by keeping the content part in the random vector while changing the motion part in the random vector. However, this method can only synthesize low resolution videos without appearance details. [40], [39] utilize the keypoint detector to extract the keypoints of the source image and the driving frame, which are used to estimate the optical flow between the source image and the driving frame. However, since these methods train the keypoint detector, dense motion network, and generator network in an end-to-end manner and there is no supervision for the keypoint detector, these methods often fail on complex human motions. Our approach can synthesize high resolution videos (1280x720) and handle complex motions, which is superior of these image animation methods.

B. Image Synthesis

Since there has been much progress in Generative Adversarial Networks (GAN) [14], image synthesis has achieved incredible results. Some works on image synthesis such as BigGAN [3] generate pictures that even humans can not distinguish them from the real images. Image synthesis can be generally classified into two categories, unconditional synthesis, and conditional synthesis. For unconditional synthesis, some work based on GAN [14] or VAE [22] learns a mapping function from noise to real image. For conditional image synthesis, conditional models usually extending Conditional Generative Adversarial Nets synthesize images given either class category, human pose, scene graphs, and another image [30], [19], [37]. Conditional Generative Adversarial Nets (C-GAN) [32] is a variant of GAN, generating images with given desired attributes by embedding conditional information on both generator and discriminator. Based on C-GAN, some works achieved an impressive result on image-to-image translation [17], [49]. Face generation plays an important role in human image synthesis. Many works are focusing on face synthesis, such as Tero Karras *et al.* [21], which have gained incredible results on face synthesis. Guha *et al.* [2] proposed a method to synthesize images of humans in unseen poses. Their method could synthesis a person's image of the desired pose via the given source image and target pose.

C. Video Synthesis

Many works on specific problems of video synthesis, including video matting and blending [1], [8], video super-resolution [36] and video inpainting [51] can be applied to other general video synthesis tasks. Among them, vid2vid [48] is a video-to-video translation framework and is capable of generating incredible high-resolution videos. Though it is possible to simply adapt this network to additionally condition on the target appearance image for our task, we show in our empirical study (section IV) that such a simple solution fails to produce satisfactory results due to the diversity of

target persons and the paucity of information provided by the single images of targets. Few-shot vid2vid [47] is the improved version of vid2vid, which aims at synthesizing video for an arbitrary person through a single model. Apart from the pose sequence, few-shot vid2vid requires some example images for the model, which can provide the appearance information of the target person. During training, it trains the vid2vid model in a few-shot paradigm. During testing, to synthesize video for a new person that does not exist in the training set, few-shot vid2vid only needs a pose sequence and few example images as the inputs of the model. Different from the above two methods, Liquid Warping GAN [28] resorts to the transformation flow between the source person and the reference person, which is used to align the feature of the source person to the target pose. The transformation flow can be obtained according to the SMPL [29] models of the source person and the reference person. Compared with the existing methods, our method incorporates the structured model and appearance flow to enable efficient structure learning and good generalization capability.

III. CPF-NET

Collaborative Parsing-Flow model (CPF-Net), integrating structured human parsing and appearance flow to guide the video synthesis, was proposed to tackle the challenges in human motion transfer. The human parsing is an effective tool for expressing the target person structure, which segments person into different parts, such as the head part and legs part. Inspired by [23], we utilize the appearance flow generated from a flow regression network to guide the synthesis of the target frame which retains most details of the appearance frame. Moreover, to fuse the foreground and background properly and keep the temporal smoothness among consecutive frames, we propose a spatio-temporal fusion network. Benefit from the collaborative structural learning guided by human parsing and flow, our approach is capable of producing photo-realistic and spatio-temporal coherent dancing videos of any target input. Figure 2 illustrates the overall architecture of our approach. We decompose the modeling into three stages which will be fully elaborated in section III-B, section III-C and section III-D respectively.

A. Problem Formulation and Notation

We consider the problem of making a target person in a static image dance like the person in a source video, by transferring motion from the source to the target. Formally, let $\mathbf{S} = \{s^1, s^2, \dots, s^T\}$ be a sequence of frames in the source dancing video, and I_a is an appearance image of the target person. Given the input pair (S, I_a) , we aim to generate a new video $\mathbf{X} = \{x^1, x^2, \dots, x^T\}$ wherein the target person performs the same dance motions as the source person. In particular, a model to the task $P(\mathbf{X}|\mathbf{S}, I_a)$ should generally apply to arbitrary source dancing video and any target person, and able to synthesize a target video that smoothly retains the motions of the source and faithfully preserve the appearance of the target.

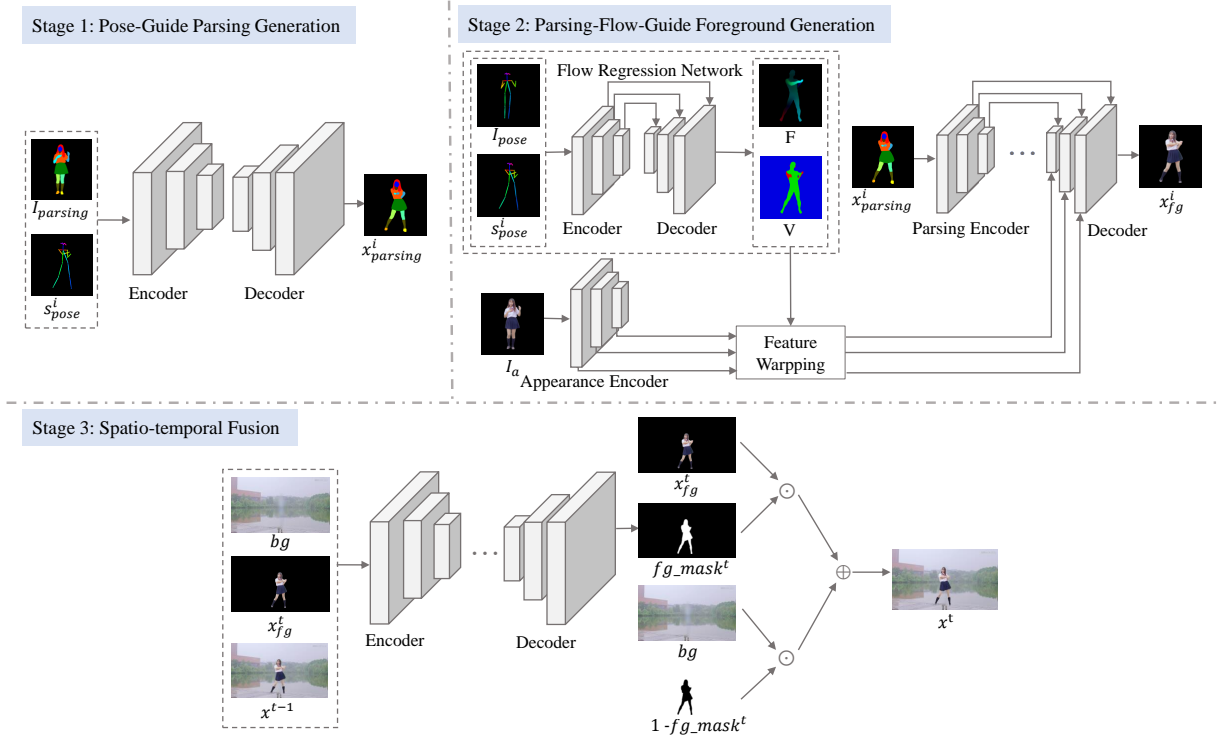


Fig. 2: **Overall architecture of the proposed CPF-Net.** In the first stage, we feed the appearance parsing $I_{parsing}^i$ and source video pose s_{pose}^i into pose-guide parsing generation module to obtain the target parsing $x_{parsing}^i$. In the second stage, appearance pose I_{pose} together with s_{pose}^i are fed into the flow regression network to obtain the appearance flow map F and visibility map V . Then the appearance foreground I_a , $x_{parsing}^i$, F and V are fed into parsing-flow-guide foreground generation module to synthesize the target foreground x_{fg}^i . In the third stage, we first extract the background from the appearance image and inpaint it as bg . Then, the inpainted background bg , current synthesized foreground x_{fg}^t and previous synthesized frame x^{t-1} are fed into spatio-temporal fusion network to obtain current foreground mask fg_mask^t , which is used to fuse x_{fg}^t and bg to synthesize the current target frame x^t .

B. Pose-Guide Parsing Generation

The first stage of CPF-Net fuses source motion with the target human structure as an intermediate representation of motion transfer. Specifically, we first apply a pre-trained pose detector on the source video frames S to extract the pose sequence S_{pose} , and apply a pre-trained human parser on the target appearance image I_a to obtain the human parsing map $I_{parsing}$.

Pose Sequence Smoothing. The predicted pose sequence S_{pose} is inevitable with some noise and these noise will cause temporal inconsistency on generated video. Therefore, Savitzky–Golay filter [43] is employed to smooth predicted pose sequence.

The goal of this stage is to generate the human parsing sequence $X_{parsing}$ of the target parsing $I_{parsing}$ that implements the source pose sequence S_{pose} :

$$X_{parsing} = G_{parsing}(S_{pose}, I_{parsing}), \quad (1)$$

where $G_{parsing}$ is a pose-guided parsing generation model.

To train the parsing generation model, we construct the training data from a set of human dancing videos. Concretely, we treat each video as the source video S , and the source subject in the video as the target person as well. A particular frame in the video is selected as the target appearance image

I_a (the selection criteria is described in Section IV-A1). In this way, the human parsing map of I_a can serve as $I_{parsing}$ of this stage and predicted parsing maps of source video frames can serve as ground true while training.

Similar to [10], we utilize the ResNet-like generator which has 9 residual blocks. The generator takes the target appearance parsing $I_{parsing}$ and pose of source video frame s_{pose}^i as inputs, and outputs the target parsing $x_{parsing}^i$ in that pose. As for loss functions, we utilize \mathcal{L}_1 loss between the generated parsing maps and ground truth parsing maps. Besides, we use a pixel-wise softmax loss \mathcal{L}_{par} from LIP [13] to improve the quality of results. Let $x_p' \in R^{W*H*C}$ and $x_p \in R^{W*H*C}$ be the predicted parsing result and parsing ground truth, where W and H denote the width and height of input image respectively and C is the number of semantic labels. Then \mathcal{L}_1 and \mathcal{L}_{par} can be formulated as below:

$$\begin{aligned} \mathcal{L}_1 &= \sum_{w=0}^W \sum_{h=0}^H \sum_{l=0}^C |x_p(w, h, l) - x_p'(w, h, l)|, \\ \mathcal{L}_{par} &= - \sum_{w=0}^W \sum_{h=0}^H \sum_{l=0}^C x_p(w, h, l) \log[x_p'(w, h, l)]. \end{aligned} \quad (2)$$

C. Parsing-Flow-Guide Foreground Generation

The second stage aims to generate a photo-realistic foreground sequence \mathbf{X}_{fg} wherein the target person dances like the person in the source video. Since the background is almost fixed, it is reasonable for the model to just focus on the foreground generation.

Because of the less appearance information in one single image, it's hard for the generator to synthesize the target frame directly while keeping the appearance details. Inspired by [23], we utilize a flow regression network to calculate the appearance flow between the source and target image and use it to warp feature maps during encoding the appearance image. The warped feature will be used during upsampling and guide the generator to synthesize details as much as possible.

Flow Regression Network. As shown in Figure 2, the flow regression network is a U-net architecture, which takes appearance pose I_{pose} and source pose s_{pose}^i as inputs, then outputs the flow map F and the visibility map V . The flow map indicates the appearance flow between the appearance image I_a and the source video frame s^i while the visibility map has three discrete values indicating whether the pixel on I_a is visible on s^i or indicating the background respectively.

Similar to [23], we calculate the ground-truth appearance flow map and visibility map with the help of the 3D model of the source image and target image. Namely, we first fit a 3D model to both source image and target image through the state-of-the-art method [20]. Then, we project the 3D model back to the 2D image plane through the image renderer [31]. Each point on the projected image has its corresponding 3D mesh face on the same 3D model. So for each point on the target projected image, our model can either find its corresponding point on the source projected image or regard it invisible on the source projected image. Based on such relation, the appearance flow map and visibility map between the source and target projected image are calculated. In our case, the source image indicates the appearance image I_a while the target image indicates the source video frame s^i .

To train this module, we take the pose pairs calculated from the projected image pairs rather than real pose pairs as input, since the 3D model fitting process may not work correctly sometimes, which results in the mismatch between the flow maps and the real pose pairs. As for loss functions, we utilize end-point-error (EPE) loss between synthetic flow map and real flow map, and cross entropy-loss between synthesized visibility map and real visibility map.

Parsing-Flow-Guide Generation Network. We utilize a dual-path U-net [34] to separately model appearance foreground and parsing map information. Different from [23], we choose the parsing map as conditional structure information. It is because the parsing map is capable of embedding more structure information of complicated motion compared to the pose map.

As illustrated in Figure 2, the parsing encoder encodes the target parsing map $x_{parsing}^i$ generated from the first stage while the appearance encoder encodes the appearance foreground I_a . Each feature map in the appearance encoder is warped according to the calculated flow map F and visibility map V . Concretely, the appearance foreground feature is

warped by the flow map. Then the warped feature map is separated into visible part and invisible part according to the visibility map. After that, these two feature maps are concatenated together and passed through two convolution layers with residual path to get final warped features. In the end, the parsing features and warped features are concatenated hierarchically which are fed into the image decoder through skip connections to generate the target foreground x_{fg}^i .

The loss functions used during training of this module are adversarial loss \mathcal{L}_{adv} , L1 reconstruction loss \mathcal{L}_{L1} and perceptual loss \mathcal{L}_{per} [18].

Following [48], adversarial loss \mathcal{L}_{adv} from discriminator can be given by utilizing the operator ϕ_I :

$$E_{\phi_I(I_a, x_{parsing}^i, x_{fg}^i)}[\log D(I_a, x_{parsing}^i, x_{fg}^i)] + E_{\phi_I(I_a, x_{parsing}^i, \hat{x}_{fg}^i)}[\log(1 - D(I_a, x_{parsing}^i, \hat{x}_{fg}^i))], \quad (3)$$

where \hat{x}_{fg}^i is the generated target foreground and x_{fg}^i is the ground truth of it.

Inspired by [18], we further improve the visual quality of generated foreground by minimizing perceptual loss. Specifically, we use a pretrained VGG19 [42] network to extract features of both the real and generated foreground, and minimizing the L1 distance between them:

$$\mathcal{L}_{per}(x_{fg}^i, \hat{x}_{fg}^i) = \sum_{i=0}^n \lambda_i \|\phi_i(x_{fg}^i) - \phi_i(\hat{x}_{fg}^i)\|_1, \quad (4)$$

in which $\phi_i(\hat{x}_{fg}^i)$ denote the i -th feature map of the synthesized image \hat{x}_{fg}^i from VGG network and λ_i denote the weight of them.

The overall loss \mathcal{L} for this stage is a weighted sum of above three loss items and λ_{adv} , λ_{L1} , λ_{per} are weights of \mathcal{L}_{adv} , \mathcal{L}_{L1} and \mathcal{L}_{per} respectively.

D. Spatio-Temporal Fusion Network

In the third stage, we propose a spatio-temporal fusion network to fuse the synthesized foreground and background properly while keeping the temporal smoothness among the consecutive frames. Briefly, given the current synthesized foreground x_{fg}^t , background bg and previous synthesized frame x^{t-1} , our model F predicts the current foreground mask fg_mask^t with a ResNet-like network, which is used to fuse foreground x_{fg}^t and background bg . Then the third stage could be formulated as:

$$fg_mask^t = F(bg, x_{fg}^t, x^{t-1}) \\ x^t = x_{fg}^t \odot fg_mask^t + bg \odot (1 - fg_mask^t). \quad (5)$$

More concretely, as shown in Figure 2, at the step of synthesizing the t -th frame x^t , we first concatenate the background bg , t -th synthesis foreground x_{fg}^t and previous synthesis frame x^{t-1} , and then feed them into a ResNet-like network which outputs a foreground mask fg_mask^t . Although the foreground generated by the second stage is photo-realistic, simply overlaying the synthesized foreground and background cannot integrate the foreground and background naturally. It's straightforward to train a model generating a mask to fuse the foreground and background. Moreover, taking the previous

synthesized frame x^{t-1} as input forces the network to focus on the previous synthesized result, which is helpful to keep the temporal smoothness.

The background used in this stage is simply inpainted by [33], refer to section IV-A1 for more details. During the training of this stage, we randomly select K consecutive frames in each video (K is set to 5 in our experiment) to represent each video. Since there is no previous synthesized frame for the first frame, we simply ignore the synthesizing of the first frame and use the directly overlaying result of the first foreground and background as the previous synthesized frame for the second frame. The loss functions used in this stage are the $L1$ reconstruction loss \mathcal{L}_{L1} and the perceptual loss \mathcal{L}_{per} [18] as shown in section III-C.

IV. EXPERIMENT

To push forward the study of human motion transfer, we construct a new large dataset for our problem (section IV-A1). We compare our approach with several strong baseline models, namely pix2pixHD [49], vid2vid [48] and soft-gated [10]. Both quantitative and qualitative results validate the significant superiority of our proposed approach.

A. Experimental Setup

1) *Datasets*: We make the first attempt to propose the Dance Motion Transfer Dataset (DMT) by collecting 428 dancing videos from a video community Bilibili. All of these videos satisfy the following key features: single person, almost fixed background, and great ranges of motions. The first two characteristics allow researchers to focus on the task of motion transfer instead of dealing with multiple persons or moving background. The third one makes our dataset close to real-life scenarios and makes the task challenging. We split our dataset into training and testing sets with 406 videos and 22 videos, respectively. The number of total frames for the training and testing sets are 561,785 and 31,680, respectively. The resolution of all videos is 1280x720.

Then, we adopted OpenPose [4], [5], [41], [50] to annotate pose keypoints of each frame. According to the problem setting, we also need to choose one appearance image for each video, which is conducted in the following way. Let (x_i^j, y_i^j, c_i^j) be the i -th keypoint information on the j -th frame, where x_i^j , y_i^j and c_i^j stand for x-coordinate, y-coordinate and confidence, respectively. A single person gets N keypoints on the body. In our case, $N = 18$. Intuitively, an appearance image should try to show every body part of a person. We thus choose the frame with the largest confidence sum as the appearance image. Moreover, we apply a pre-trained human parser [11] to get the parsing map of each video frame. Since the foreground occupies only a small portion of the entire image, we crop a small rectangle region containing the foreground according to the parsing map and record the coordinates of the rectangle in the original image. After padding and resize, the crop foreground size becomes $448 * 448$, which is the image size for the first and second stages. In the third stage, the cropped image is restored to its original size based on its cropped coordinates. Similarly, we crop the human

out from the appearance image and inpaint the remaining incomplete background with EdgeConnect [33]. Then, the inpainted results will serve as background of each video.

Comparing with other similar datasets, such as iPER [28], DMT consists of more than ten times distinct subjects and a much larger diversity of motions which brings more challenges and complexity and also brings greater possibilities for practical application. Besides, their dataset is splitted by different clothes while our dataset is splitted by different subjects.

2) *Comparison Methods*: As discussed below, we selected a wide range of methods as the baselines on this work. Pix2pixHD [49] and vid2vid [48] are SOTA image2image synthesis and video2video synthesis framework respectively, and the soft-gated warping GAN [10] is the latest human synthesis framework. Few-shot vid2vid [47] and liquid warping GAN [28] are latest few-shot video2video synthesis frameworks, which can synthesize videos according to single image. The implementation details of these methods are as follows. **Pix2pixHD** [49] takes an image as input and also output one image. We made some adaptation about pix2pixHD to apply it to our task setting. Concretely, we concatenate the target pose, the appearance image and the previous L generated frames $X^{t-L,t-1}$ together on the channel as input to pix2pix then compute the final t -th output frame.

Vid2vid [48]. Similar to our experiment on pix2pixHD, we concatenate the appearance image with each frame of the target pose video and feed it to the vid2vid framework to get the resulted video so that it can conditioned on the extra appearance image.

Soft-Gated Warping GAN [10] was proposed to solve the pose-guided person image synthesis problem. Given the target pose and appearance image, it can generate a realistic person image with target pose while preserving the appearance of the target person. A frame-by-frame soft-gated warping GAN is employed as one of our baseline methods.

Few-shot vid2vid [47]. The inputs consist of a pose sequence and some examples images. In our task setting, only one appearance frame is provided. Therefore, the appearance image is regarded as the only example image for the few-shot vid2vid model.

Liquid Warping GAN [28]. The setting of the Liquid Warping GAN is a bit different from our task, since one of the inputs of the model is the video sequence rather than the pose sequence. Thus, during training or testing, we regard the appearance image and the target frame which corresponds to the target pose from the same video as the inputs of the model.

3) *Implementation Details*: During training, adam optimization is used for three stages with $(\beta_1 = 0.5, \beta_2 = 0.999)$. As for the first stage, the initial learning rate is set to 0.0002. The weight for two losses in this stage is equally set to 10.0. The high-quality parsing result can be obtained within 30 epochs of training. During training the second stage, generator and discriminator are updated alternatively with batch size 8. Learning rates for generator and discriminator are initialized to 0.0002 and 0.00002 respectively. We set $\{\lambda_{adv}, \lambda_{L1}, \lambda_{per}\} = \{0.01, 1.0, 1.0\}$. We can get realistic and natural results within 40 epochs. During training the last stage, the learning rate is initialized to 0.0001 and the batch size is

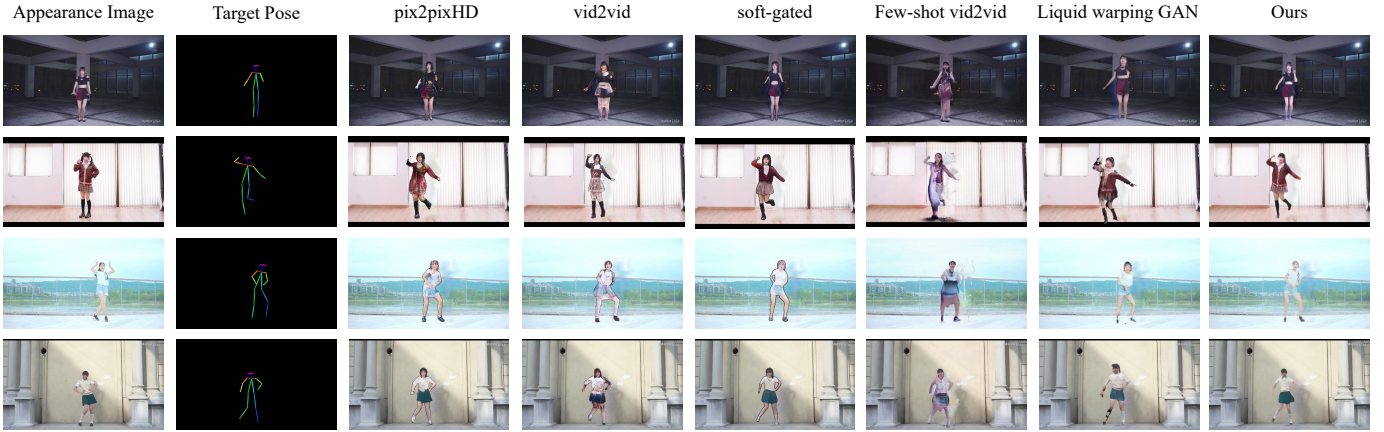


Fig. 3: **Visual comparison between our method and baseline methods on DMT dataset.** The first column is input appearance images and the second column is the target pose we want to synthesize. Our method provides more photo-realistic results than baseline methods. Please zoom in for better view.

set to 1 because of the high-resolution image. The loss weights are equally set to 1.0. We can obtain the natural results within 5 epochs.

Method	Fréchet Video Distance
pix2pixHD [49]	1783.94
vid2vid [48]	2244.97
soft-gated [10]	1555.33
Few-shot vid2vid [47]	1608.80
Liquid Warping GAN [28]	2345.90
Ours (w/o appearance flow)	1285.68
Ours (w/o fusion module)	1454.47
Ours	1005.84

TABLE I: **Comparison of Fréchet Video Distance between our method and baselines on DMT dataset.** The lower is the better.

Comparison Method Pair	Human Eval Score
Ours vs pix2pixHD [49]	0.94 vs 0.06
Ours vs vid2vid [48]	0.98 vs 0.02
Ours vs soft-gated [10]	1.00 vs 0.00
Ours vs Ours (w/o appearance flow)	0.88 vs 0.12
Ours vs Ours (w/o fusion module)	0.95 vs 0.05
Ours (F) vs pix2pixHD (F) [49]	0.93 vs 0.07
Ours (F) vs vid2vid (F) [48]	0.96 vs 0.04
Ours (F) vs soft-gated (F) [10]	0.88 vs 0.12

TABLE II: **Human evaluation results comparing pairs of methods on DMT dataset.**(F) means that only generated foreground is used for evaluation.

Method	Fréchet Video Distance
Liquid Warping GAN [28]	1134.48
Ours	1083.62

TABLE III: **Comparison of Fréchet Video Distance between our method and Liquid Warping GAN [28] on iPER dataset.** The lower is the better.

B. Quantitative Results

Fréchet Video Distance (FVD) [45] is a new metric for generative models of video based on Fréchet Inception Distance (FID) [16]. This metric considers both temporal consistency and visual quality of each frame with the lower score representing the better result. [45] conducted a large-scale human study and confirmed that FVD correlates well with qualitative human judgment of those generated videos. On our evaluation, the network used to calculate FVD is I3D [6]. We calculate FVD between source videos of test set and generated videos. Corresponding to the released code of FVD, we selected 30 consecutive frames of each video to calculate the FVD.

Table I shows the comparison results among our method and the other three baselines. We can observe that our method gets the lowest FVD score. The FVD score of soft-gated [10], Few-shot vid2vid [47], Liquid Warping GAN [28], pix2pixHD [49] and vid2vid [48] ranks in increasing order. The videos generated by vid2vid [48] get the largest distance among all methods. Pix2pixHD [49] and soft-gated [10] focus more on synthesis of single frame while vid2vid [48] pays more attention to the fluency of video, which may cause degradation on generated videos of vid2vid [48]. Table III shows the comparison results among our method and Liquid Warping GAN [28] on iPER dataset. We can observe that our method gets the lower FVD score than Liquid Warping GAN, and this illustrates that our method is of good generalization.

C. Human Evaluation

For video synthesis tasks, human evaluation is always the most accurate and reliable. We conduct our human evaluation on Amazon Mechanical Turk. In each test, we provide two videos (about 10 seconds) to each participant, in which one comes from the compared method (baseline method or ablation method) and the other comes from our proposed method. The expectation for them is to choose the more realistic and natural video from the two. All videos of the test set are used for evaluation and each video will be evaluated by 5 independent

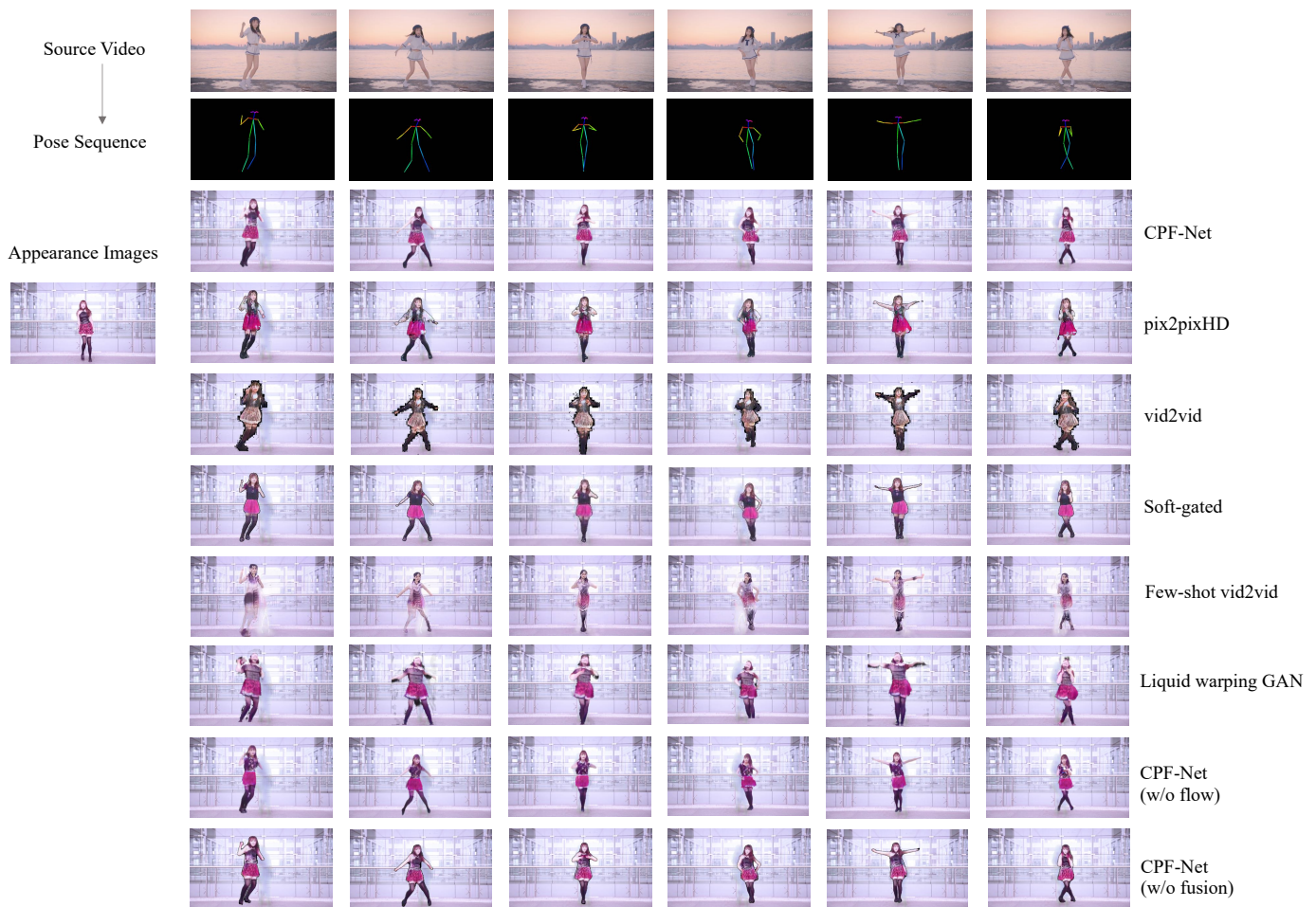


Fig. 4: **Consecutive results on the test set.** The first row and second row are source video and estimated pose sequence respectively. The following rows are synthesized videos from CPF-Net, pix2pixHD, vid2vid, soft-gated, Few-shot vid2vid, Liquid warping GAN, CPF-Net(w/o appearance flow) and CPF-Net(w/o Spatio-temporal fusion) in sequence.

workers. To ensure the accuracy of test results, we require the workers to be master qualified by Amazon.

The human evaluation results among our method and the other three baselines are demonstrated in Table II. Our method shows absolute superiority in authenticity and naturalness by ratio 0.94, 0.98, 1.00 compared to baselines pix2pixHD [49], vid2vid [48] and soft-gated [10]. To further evaluate our proposed method on foreground generation, human evaluation with foreground videos was conducted. Our approach still outperforms with the three baseline methods with 0.93, 0.96 and 0.88 on foreground generation respectively. To sum up, videos generated by our model have significantly better visual quality from the perspective of a human.

D. Qualitative Results

We first compare the motion transfer results of baselines and our method in the single frame, as shown in Figure 3. Obviously, our method acquires better results both on clothes detail retention and human outline. The visual qualities of pix2pixHD [49] and vid2vid [48] are poorer than the other three methods. This owes to the simple synthesizing from the generator, resulting in the lack of appearance details and

some wrong appearance synthesis. Human images generated by soft-gated [10] and liquid warping GAN [28] seem better than the other three baselines due to their warping operation. However, our method still outperforms soft-gated, where the enlarged images in Figure 6 shows our method maintains better facial details as well as clothing texture. Additionally, we also provide the consecutive results of generated videos of our method and baselines in Figure 4. Similar to the single frame, our method performs better in transferring poses and retaining the details of appearance. Figure 5 shows the visual comparison between our proposed method and liquid warping GAN [28] on iPER dataset. Our proposed method achieved better visual quality than liquid warping GAN, and this verified the generality of our proposed method.

E. Ablation Study

We conduct two additional experiments to verify the effectiveness of different modules in CPF-Net, namely CPF-Net without using appearance flow and CPF-Net without spatio-temporal fusion. The implementation details of these ablation methods are as follows.

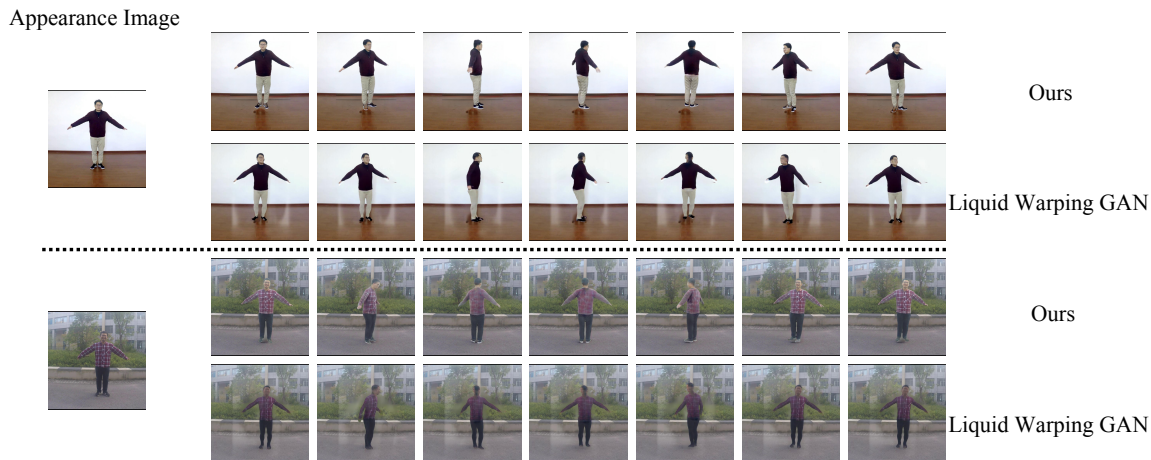


Fig. 5: **Vision comparison between our method and Liquid Warping GAN [28] on iPER dataset.** All models are trained with iPER dataset.

CPF-Net(w/o flow). Flow Regression Network of second stage is not used. The feature map extracted from the appearance foreground I_a is directly fed into the image decoder without feature warping.

CPF-Net(w/o fusion). Mask fg_{mask}^t generated by Spatio-Temporal Fusion Network is not used. Generated parsing map $x_{parsing}^i$ is directly used as mask to fuse foreground and background.

The results of FVD are shown in Table I, while some visual results are presented in Figure 4. The full model of CPF-Net obtains the best score of FVD compared to the other two methods, which indicates each module of proposed CPF-Net is essential for the synthesized video. Moreover, the FVD score of CPF-Net without spatio-temporal fusion module still outperforms the baselines, which demonstrates the visual quality of the single frame generated by the second stage is better than the other baselines. As shown in Figure 4, the synthesized frames generated by CPF-Net without using appearance flow usually lack of appearance details. CPF-Net without spatio-temporal fusion module can not integrate the foreground and background naturally, which usually generates a boundary between the foreground and background. Moreover, Table II shows that videos generated by the full model of CPF-Net gains a much higher score on human evaluation than ablation models which means much better visual quality is gained by full model. To sum up, both subjective and objective metric show the necessity of each part of CPF-Net.

V. CONCLUSION

In this work, we introduce a more general motion transferring task where we aim to learn a single model to parsimoniously transfer motion from a source video to any target person given only one image of the target. We propose a structured approach, named as Collaborative Parsing-Flow Video Synthesis (CPF-Net), to guide the synthesis of photo-realistic foreground, which will be merged into the background by a spatio-temporal fusion module. The problem is decoupled into stages of human parsing generation, photo-realistic foreground generation, and temporal consistent video

generation. We demonstrate the integration of human parsing map and appearance flow bring a large improvement to the visual quality in the final video while the spatio-temporal fusion module guarantees the natural fusion of foreground and background and the temporal smoothness of the synthesis video. We conduct comparison experiments with a wide range of baseline methods, both quantitative results and qualitative results demonstrate the superiority of our method.

ACKNOWLEDGMENTS

This work was supported in part by National Key R&D Program of China under Grant No. 2020AAA0109700, National Natural Science Foundation of China (NSFC) under Grant No.U19A2073 and No.61976233, Guangdong Province Basic and Applied Basic Research (Regional Joint Fund-Key) Grant No.2019B1515120039, Guangdong Outstanding Youth Fund (Grant No. 2021B1515020061), Shenzhen Fundamental Research Program (Project No. RYX20200714114642083, No. JCYJ20190807154211365), CSIG Youth Fund.

REFERENCES

- [1] Xue Bai, Jue Wang, David Simons, and Guillermo Sapiro. Video snapcut: robust video object cutout using localized classifiers. In *SIGGRAPH '09*, 2009.
- [2] Guha Balakrishnan, Amy Zhao, Adrian V. Dalca, Frédo Durand, and John V. Guttag. Synthesizing images of humans in unseen poses. *2018 IEEE/CVF Conference on Computer Vision and Pattern Recognition*, pages 8340–8348, 2018.
- [3] Andrew Brock, Jeff Donahue, and Karen Simonyan. Large scale gan training for high fidelity natural image synthesis. *CoRR*, abs/1809.11096, 2018.
- [4] Z. Cao, G. Hidalgo Martinez, T. Simon, S. Wei, and Y. A. Sheikh. Openpose: Realtime multi-person 2d pose estimation using part affinity fields. *IEEE Transactions on Pattern Analysis and Machine Intelligence*, 2019.
- [5] Zhe Cao, Tomas Simon, Shih-En Wei, and Yaser Sheikh. Realtime multi-person 2d pose estimation using part affinity fields. In *CVPR*, 2017.
- [6] J. Carreira and A. Zisserman. Quo vadis, action recognition? a new model and the kinetics dataset. *CVPR*, 2017.
- [7] Caroline Chan, Shiry Ginosar, Tinghui Zhou, and Alexei A Efros. Everybody dance now. *arXiv preprint arXiv:1808.07371*, 2018.
- [8] Tao Chen, Jun-Yan Zhu, Ariel Shamir, and Shimin Hu. Motion-aware gradient domain video composition. *IEEE Transactions on Image Processing*, 22:2532–2544, 2013.

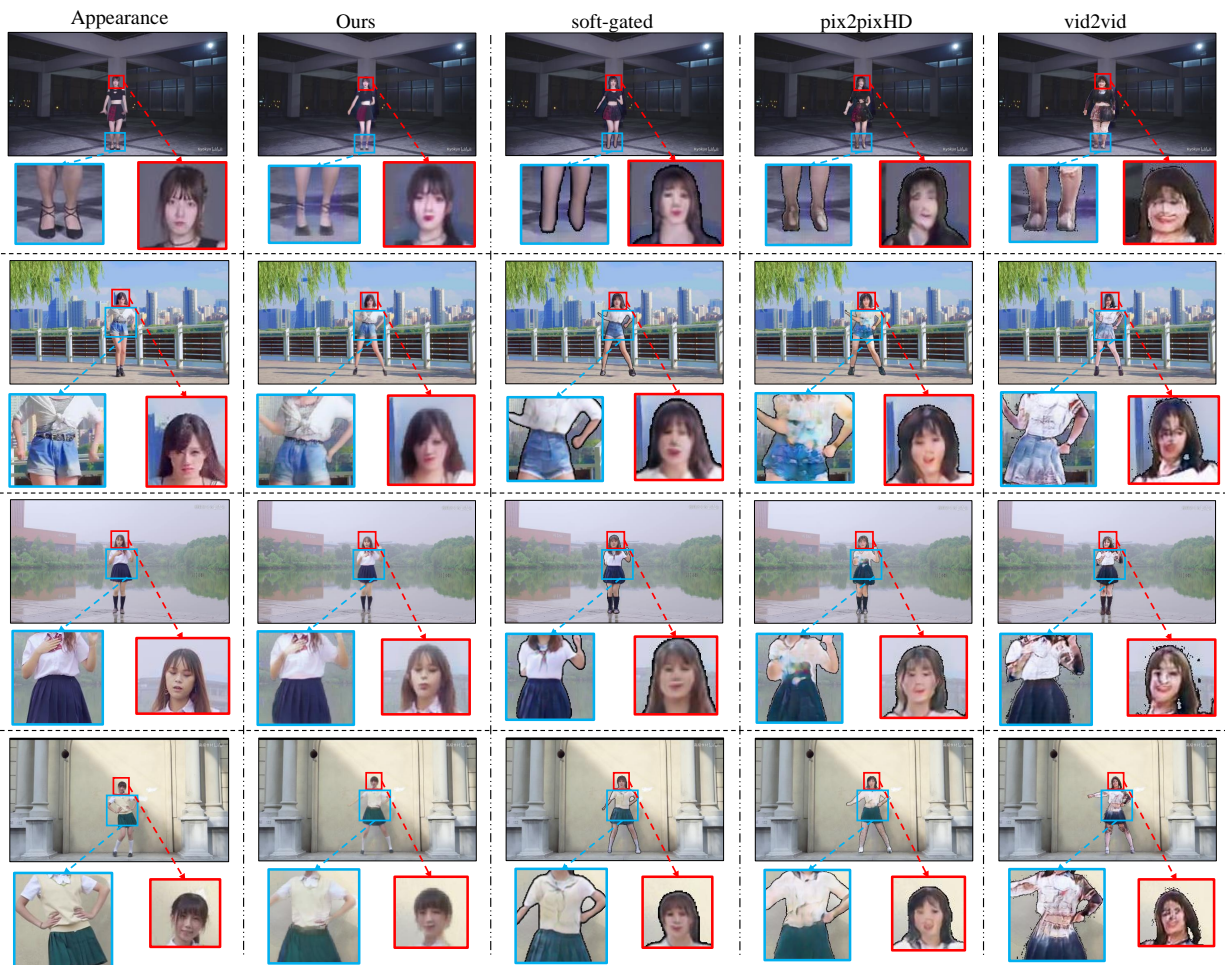


Fig. 6: **Detail comparison between our method and baseline methods.** The images on the first column are input appearance images and the images lies on the second column are generated by our method and the images lies on the remaining columns are generated by baseline methods. The enlarged detail images illustrate that CPF-Net is capable to generate much more face details(e.g., cleaner hair)and much better clothes texture than baseline methods.

- [9] German KM Cheung, Simon Baker, Jessica Hodgins, and Takeo Kanade. Markerless human motion transfer. In *Proceedings. 2nd International Symposium on 3D Data Processing, Visualization and Transmission, 2004. 3DPVT 2004.*, pages 373–378. IEEE, 2004.
- [10] Haoye Dong, Xiaodan Liang, Ke Gong, Hanjiang Lai, Jia Zhu, and Jian Yin. Soft-gatedwarping-gan for pose-guided person image synthesis. In *NeurIPS*, 2018.
- [11] Ke Gong, Yiming Gao, Xiaodan Liang, Xiaohui Shen, Meng Wang, and Liang Lin. Graphonomy: Universal human parsing via graph transfer learning. 2019.
- [12] Ke Gong, Xiaodan Liang, Yicheng Li, Yimin Chen, Ming Yang, and Liang Lin. Instance-level human parsing via part grouping network. In *ECCV*, pages 770–785, 2018.
- [13] Ke Gong, Xiaodan Liang, Xiaohui Shen, and Liang Lin. Look into person: Self-supervised structure-sensitive learning and a new benchmark for human parsing. *CVPR*, 2017.
- [14] Ian J. Goodfellow, Jean Pouget-Abadie, Mehdi Mirza, Bing Xu, David Warde-Farley, Sherjil Ozair, Aaron Courville, and Yoshua Bengio. Generative Adversarial Networks. *arXiv e-prints*, page arXiv:1406.2661, Jun 2014.
- [15] Chris Heckler, Bernd Raabe, Ryan W Enslow, John DeWeese, Jordan Maynard, and Kees van Prooijen. Real-time motion retargeting to highly varied user-created morphologies. In *ACM Transactions on Graphics (TOG)*, volume 27, page 27. ACM, 2008.
- [16] Martin Heusel, Hubert Ramsauer, Thomas Unterthiner, Bernhard Nessler, and Sepp Hochreiter. Gans trained by a two time-scale update rule converge to a local nash equilibrium. In *NIPS*, 2017.
- [17] Phillip Isola, Jun-Yan Zhu, Tinghui Zhou, and Alexei A Efros. Image-to-image translation with conditional adversarial networks. *CVPR*, 2017.
- [18] Justin Johnson, Alexandre Alahi, and Li Fei-Fei. Perceptual losses for real-time style transfer and super-resolution. In *ECCV*, pages 694–711, 2016.
- [19] Justin Johnson, Agrim Gupta, and Li Fei-Fei. Image generation from scene graphs. In *CVPR*, pages 1219–1228, 2018.
- [20] Angjoo Kanazawa, Michael J Black, David W Jacobs, and Jitendra Malik. End-to-end recovery of human shape and pose. *CVPR*, 2018.
- [21] Tero Karras, Timo Aila, Samuli Laine, and Jaakko Lehtinen. Progressive growing of gans for improved quality, stability, and variation. *CoRR*, abs/1710.10196, 2017.
- [22] Diederik P Kingma and Max Welling. Auto-encoding variational bayes. *arXiv preprint arXiv:1312.6114*, 2013.
- [23] Yining Li, Chen Huang, and Chen Change Loy. Dense intrinsic appearance flow for human pose transfer. *CVPR*, 2019.
- [24] Xiaodan Liang, Ke Gong, Xiaohui Shen, and Liang Lin. Look into person: Joint body parsing & pose estimation network and a new benchmark. *IEEE transactions on pattern analysis and machine intelligence*, 2018.
- [25] Xiaodan Liang, Xiaohui Shen, Donglai Xiang, Jiashi Feng, Liang Lin, and Shuicheng Yan. Semantic object parsing with local-global long short-term memory. In *CVPR*, pages 3185–3193, 2016.
- [26] Xiaodan Liang, Chunyan Xu, Xiaohui Shen, Jianchao Yang, Si Liu, Jinhui Tang, Liang Lin, and Shuicheng Yan. Human parsing with contextualized convolutional neural network. In *ICCV*, pages 1386–1394, 2015.

- [27] Lingjie Liu, Weipeng Xu, Michael Zollhöfer, Hyeonwoo Kim, Florian Bernard, Marc Habermann, Wenping Wang, and Christian Theobalt. Neural animation and reenactment of human actor videos. *ArXiv*, abs/1809.03658, 2018.
- [28] Wen Liu, Zhixin Piao, Jie Min, Wenhan Luo, Lin Ma, and Shenghua Gao. Liquid warping gan: A unified framework for human motion imitation, appearance transfer and novel view synthesis. *ArXiv*, abs/1909.12224, 2019.
- [29] Matthew Loper, Naureen Mahmood, Javier Romero, Gerard Pons-Moll, and Michael J. Black. Smpl: a skinned multi-person linear model. *ACM Trans. Graph.*, 34:248:1–248:16, 2015.
- [30] Liqian Ma, Xu Jia, Qianru Sun, Bernt Schiele, Tinne Tuytelaars, and Luc Van Gool. Pose guided person image generation. In *NIPS*, pages 406–416, 2017.
- [31] MatthewMLoper and Michael J Black. Opendr: An approximate differentiable renderer. *ECCV*, 2014.
- [32] Mehdi Mirza and Simon Osindero. Conditional generative adversarial nets. *CoRR*, abs/1411.1784, 2014.
- [33] Kamyar Nazeri, Eric Ng, Tony Joseph, Faisal Z. Qureshi, and Mehran Ebrahimi. Edgeconnect: Generative image inpainting with adversarial edge learning. *ICCV*, 2019.
- [34] Olaf Ronneberger and Philipp Fischer and Thomas Brox. U-net:convolutional networks for biomedical image segmentation. *MIC-CAI*, 2015.
- [35] Ju Shen and Jianjun Yang. Automatic pose tracking and motion transfer to arbitrary 3d characters. In *International Conference on Image and Graphics*, pages 640–653. Springer, 2015.
- [36] Wenzhe Shi, Jose Caballero, Ferenc Huszár, Johannes Totz, Andrew P. Aitken, Rob Bishop, Daniel Rueckert, and Zehan Wang. Real-time single image and video super-resolution using an efficient sub-pixel convolutional neural network. *2016 CVPR*, pages 1874–1883, 2016.
- [37] Ashish Shrivastava, Tomas Pfister, Oncel Tuzel, Joshua Susskind, Wenda Wang, and Russell Webb. Learning from simulated and unsupervised images through adversarial training. In *CVPR*, pages 2107–2116, 2017.
- [38] Aliaksandra Shysheya, Egor Zakharov, Kara-Ali Aliev, R S Bashirov, Egor Burkov, Karim Isakov, Aleksei Ivakhnenko, Yury Malkov, I. M. Pasechnik, Dmitry Ulyanov, Alexander Vakhitov, and Victor S. Lempitsky. Textured neural avatars. In *CVPR*, 2019.
- [39] Aliaksandr Siarohin, Stéphane Lathuilière, S. Tulyakov, E. Ricci, and N. Sebe. Animating arbitrary objects via deep motion transfer. *2019 IEEE/CVF Conference on Computer Vision and Pattern Recognition (CVPR)*, pages 2372–2381, 2019.
- [40] Aliaksandr Siarohin, Stéphane Lathuilière, S. Tulyakov, E. Ricci, and N. Sebe. First order motion model for image animation. In *NeurIPS*, 2019.
- [41] Tomas Simon, Hanbyul Joo, Iain Matthews, and Yaser Sheikh. Hand keypoint detection in single images using multiview bootstrapping. In *CVPR*, 2017.
- [42] Karen Simonyan and Andrew Zisserman. Very deep convolutional networks for large-scale image recognition. *CoRR*, abs/1409.1556, 2015.
- [43] J. Steinier, Yves Termonia, and Jean jacques Deltour. Smoothing and differentiation of data by simplified least square procedure. *Analytical chemistry*, 44 11:1906–9, 1964.
- [44] Sergey Tulyakov, Ming-Yu Liu, Xiaodong Yang, and Jan Kautz. Mocogan: Decomposing motion and content for video generation. *2018 CVPR*, pages 1526–1535, 2018.
- [45] Thomas Unterthiner, Sjoerd van Steenkiste, Karol Kurach, Raphael Marinier, Marcin Michalski, and Sylvain Gelly. Towards accurate generative models of video: A new metric & challenges. *arXiv preprint arXiv:1812.01717*, 2018.
- [46] Ruben Villegas, Jimei Yang, Duygu Ceylan, and Honglak Lee. Neural kinematic networks for unsupervised motion retargetting. In *CVPR*, pages 8639–8648, 2018.
- [47] T. Wang, Ming-Yu Liu, A. Tao, Guilin Liu, J. Kautz, and Bryan Catanzaro. Few-shot video-to-video synthesis. *ArXiv*, abs/1910.12713, 2019.
- [48] Ting-Chun Wang, Ming-Yu Liu, Jun-Yan Zhu, Guilin Liu, Andrew Tao, Jan Kautz, and Bryan Catanzaro. Video-to-video synthesis. In *NeurIPS*, 2018.
- [49] Ting-Chun Wang, Ming-Yu Liu, Jun-Yan Zhu, Andrew Tao, Jan Kautz, and Bryan Catanzaro. High-resolution image synthesis and semantic manipulation with conditional gans. In *CVPR*, 2018.
- [50] Shih-En Wei, Varun Ramakrishna, Takeo Kanade, and Yaser Sheikh. Convolutional pose machines. In *CVPR*, 2016.
- [51] Yonatan Wexler, Eli Shechtman, and Michal Irani. Space-time completion of video. *IEEE Transactions on Pattern Analysis and Machine Intelligence*, 29, 2007.
- [52] Qixian Zhou, Xiaodan Liang, Ke Gong, and Liang Lin. Adaptive temporal encoding network for video instance-level human parsing. *arXiv preprint arXiv:1808.00661*, 2018.



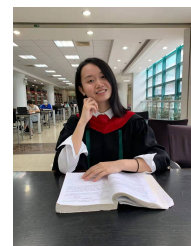
Bowen Wu received his BE degree and is currently working toward the ME degree in the School of Data and Computer Science, Sun Yat-sen University, China. His research interests include generative model and its applications.



Zhenyu Xie received his bachelor degree from Sun Yat-sen University and is studying for the master degree in the School of Data and Computer Science, Sun Yat-sen University. Currently, his research interests consist of image synthesis and video synthesis.



Xiaodan Liang is currently an Associate Professor at Sun Yat-sen University. She was a postdoc researcher in the machine learning department at Carnegie Mellon University, working with Prof. Eric Xing, from 2016 to 2018. She received her PhD degree from Sun Yat-sen University in 2016, advised by Liang Lin. She has published several cutting-edge projects on human-related analysis, including human parsing, pedestrian detection and instance segmentation, 2D/3D human pose estimation and activity recognition.



Yubei Xiao received her BE degree and is currently working toward the ME degree in the School of Data and Computer Science, Sun Yat-sen University, China. Her research interests include unsupervised learning and meta-learning for speech recognition.



Haoye Dong is a Ph.D student at School of Data and Computer Science, Sun Yat-sen University, advised by Prof. Jian Yin. He received his master degree from School of Computer Science, South China Normal University in 2016, advised by Prof. Yong Tang. He received his bachelor degree from School of Computer Science, Guangdong Polytechnic Normal University in 2012. His research interests are deep generative learning and human-centric image/video synthesis.



Liang Lin is CEO of DMAI Great China and a full professor of Computer Science in Sun Yat-sen University. He served as the Executive Director of the SenseTime Group from 2016 to 2018, leading the R&D teams in developing cutting-edge, deliverable solutions in computer vision, data analysis and mining, and intelligent robotic systems. He has authored or co-authored more than 200 papers in leading academic journals and conferences (e.g., TPAMI/IJCV, CVPR/ICCV/NIPS/ICML/AAAI). He is an associate editor of IEEE Trans, Human-Machine Systems and

IET Computer Vision, and he served as the area/session chair for numerous conferences, such as CVPR, ICME, ICCV, ICMR. He was the recipient of Annual Best Paper Award by Pattern Recognition (Elsevier) in 2018, Dimond Award for best paper in IEEE ICME in 2017, ACM NPAR Best Paper Runners-Up Award in 2010, Google Faculty Award in 2012, award for the best student paper in IEEE ICME in 2014, and Hong Kong Scholars Award in 2014. He is a Fellow of IET.